CO adsorption on the CO-precovered Pt(111) surface characterized by density-functional theory

J. A. Steckel,* A. Eichler, and J. Hafner
Institut für Materialphysik and Center for Computational Materials Science, Universität Wien, Sensengasse 8/12, A-1090 Wien, Austria
(Received 13 March 2003; published 29 August 2003)

Ab initio density-functional investigations of the gradual adsorption of increasing amounts of CO on partially precovered Pt(111) surfaces are presented. Our calculations show that up to precoverages as high as 0.5 monolayer (ML) CO, the adsorption energy is minimally influenced by lateral interactions and that adsorption of additional CO molecules remains an unactivated process. The saturation coverage is estimated to be ~ 0.67 ML. Beyond this limit the adsorption energies are strongly reduced and substantial barriers against further adsorption are built up. For the high-coverage limit, we have examined several adsorption geometries proposed in the literature as well as a novel configuration. Energetic considerations, the calculated adsorption geometries, and the analysis of the calculated frequency spectra all favor a model with the $c(\sqrt{3}\times 3)$ periodicity as proposed on the basis of the experimental data.

DOI: 10.1103/PhysRevB.68.085416 PACS number(s): 68.35.Ja, 68.43.−h, 82.45.Jn

I. INTRODUCTION

There is a long and rich history of research of the interaction of CO with platinum surfaces. Surface reactions involving CO, such as the oxidation of CO to form CO_2, are technologically and industrially important. Platinum is considered a ''prototype'' catalyst and reactions on platinum surfaces are of critical importance in the development of catalysts for diverse applications from pollution controls for the automotive industry to Fischer-Tropsch synthesis.

Recent developments have prompted new interest in the study of platinum catalysts. In particular, hydrogen-powered polymer electrolyte membrane (PEM) fuel cells show much promise as an efficient, clean, energy conversion method. As there are unsolved problems related to the storage of the hydrogen fuel, onboard production of hydrogen (from natural gas or methanol) is being explored as a method to provide H_2 fuel. In the case that onboard production of H_2 fuel is provided by steam reforming or similar methods, the gas mixture would contain significant amounts of other gases such as CO and H_2O. Unfortunately, PEM fuel cells are contaminated by CO levels as low as 100 ppm. Effective methods for the removal of CO in the presence of high concentrations of H_2 would be of tremendous value to the fuel cell industry. For this application, an ideal catalyst would oxidize CO but not H_2.

Schubert and co-workers have used diffuse reflectance Fourier transform infrared spectroscopy to study preferential oxidation of CO in H_2-rich gas over two catalysts: $Pt/\gamma-Al_2O_3$ and $Au/\alpha-Fe_2O_3$.[1] The experiments were carried out at the envisaged operating temperatures for each catalyst (200 and 80 °C, respectively). The selectivity of the two catalysts differ markedly. The selectivity of the gold catalyst decreases with decreasing CO concentration and increasing temperature. The selectivity of the platinum catalyst, while lower than that of the gold catalyst, remains unaffected by changes in CO concentration or increases in temperature. Schubert and coworkers postulate that the differences in specificity of the two catalysts are related to differences in the CO coverage on the surface. Specifically, they postulate that the gold catalyst operates at low CO coverage while the platinum catalyst operates at essentially a saturation coverage at the projected operating conditions of the feed stream.[1]

While much theoretical work has focused on the adsorption and oxidation of CO on bare Pt(111),[2–10] less is known about these processes on the CO-precovered Pt(111) surface. Our goal in the present study is to describe, using density functional theory, the potential energy profile for a CO molecule approaching the Pt(111) surface with varying amounts of CO precoverage. We have included calculations of adsorption at low coverage, but the main focus is on possible scenarios for adsorption at 0.5 ML and above.

It has been shown that well-converged DFT calculations (using typical exchange correlation functionals such as Perdew Wang 91) predict incorrect CO binding energies for high symmetry sites on Pt(111), namely, the high-coordination hollow sites are favored over the bridge sites, which are in turn favored over the top sites, in contradiction with experimental evidence supporting a site preference for atop bonding at low coverage and atop plus bridge bonding at higher coverage.[8–11] The use of the revised Perdew-Burke-Ernzerhof (RPBE) functional[12] has been found to result in better absolute CO binding energies as well as a reduction in the erroneous energy preference for the fcc hollow site on the Pt(111) surface, and the use of the projector augmented wave (PAW) method[13,14] in place of ultrasoft pseudopotentials results in a similar improvement.[8,12]

Gil and co-workers have shown that hybrid functionals that include a portion of the exact exchange provide a degree of stabilization of the atop CO with respect to hollow-site-bonded CO molecules and they argue that the energetic preference for the hollow site is due to an inadequate description of the gap between the highest occupied and lowest unoccupied molecular orbitals (HOMO-LUMO gap).[10] Kresse has reasoned that overestimation of the interaction between the LUMO and the metal substrate lowers particularly the adsorption energy for CO at the hollow site because it is at the hollow site where the LUMO-metal substrate interaction is most dominant and has shown that arbitrarily raising the energy of the unoccupied bands to higher energies leads to an

energetic preference for the top site, in agreement with experiment.[11]

It is important to note that the site preference problem does not imply that DFT is of no value for the the study of chemisorption of CO on Pt(111).[8] Because we deliberately avoid making comparisons between adsorption energies of structures that have differing ratios of top to bridge to hollow-bonded CO molecules, the site preference problem should not preclude the validity of the present results.

II. EXPERIMENTAL STUDIES

The adsorption of CO on Pt(111) has been studied with a variety of experimental techniques. For the limit of zero coverage, calorimetric studies on single crystals lead to measured heats of adsorption near 1.40 eV,[15–17] although temperature programed desorption studies have yielded slightly lower values, e.g., 1.26 eV (Ref. 18) and 1.35 eV,[19] and calorimetric studies on thin films have yielded values near 1.94 eV.[20,21] It has been demonstrated that as CO coverage increases, there is trend of decreasing heat of desorption.[20,22]

At low coverage, only top sites are occupied as evidenced by a single infrared (IR) absorbance near 2090 cm^{-1}.[23] At a CO coverage of about 0.33 ML, the IR peak moves upward to near 2100 cm^{-1} and this has been associated with atop CO molecules in a partially ordered $(\sqrt{3}\times\sqrt{3})$ R30° structure [as evidenced by slightly fuzzy low energy electron diffraction (LEED) patterns].[24–26]

At half-monolayer coverage, LEED studies reveal a well-ordered $c(4\times2)$ pattern.[23,24,27,28] The IR peak at 2100 cm^{-1} is joined by another peak near 1870 cm^{-1}.[23,24,26,29] The peak at 2100 cm^{-1} is attributed to atop CO molecules and that at 1870 cm^{-1} to bridge-bonded CO molecules. As the $c(4\times2)$ structure develops, the 1870 cm^{-1} peak attains 85% of the intensity of the peak at 2100 cm^{-1}.[24] Results of several spectroscopic, scanning tunneling microscope, and photoelectron diffraction studies are consistent with a configuration with half the CO molecules on bridge and half on top sites.[7,24,27,30] The description of the $c(4\times2)$-2CO phase was refined by automated tensor LEED.[31] The CO molecules are perpendicular to the surface, and CO bond lengths are 1.12 and 1.19 $\pm$ 0.04 Å for top and bridge-bonded molecules, respectively. The Pt atoms that support CO molecules are lifted slightly out of the plane of the surface and this leads to a small tendency towards buckling in the top layer.[31]

In 1981, based on the results of electron energy loss spectroscopy (EELS) experiments, Avery proposed a structural model for chemisorption above 0.5 ML that accounts for the higher coverage by fault lines of closely packed (full monolayer) atop-CO species separating antiphase domains of c(4×2) CO species.[24] In Fig. 1, the $(\sqrt{3}\times5)$rect and $(\sqrt{3}\times3)$rect models suggested by Avery are depicted; they correspond to coverages of 0.6 and 0.667 ML, respectively. The surface cells have one side with a constant length of $\sqrt{3}$ while the other side has a variable length. Further evidence for dense CO layers on Pt(111) and the $(\sqrt{3}\times5)$rect and $(\sqrt{3}\times3)$rect models is provided by the high resolution EELS, temperature programed desorption and LEED results of Kostov *et al.* and Biberian *et al.*[26,29] According to Avery's model, as surface crowding occurs, the proportion of atop CO molecules increases relative to the proportion of bridge-bonded species. This is supported by EELS data showing that as coverage increases, the 2100 cm^{-1} peak loses 20% of its intensity and the 1870 cm^{-1} peak loses 50% of its intensity.[24] Coverage increases as spacing decreases between the fault lines, until saturation is reached at 0.667 ML.

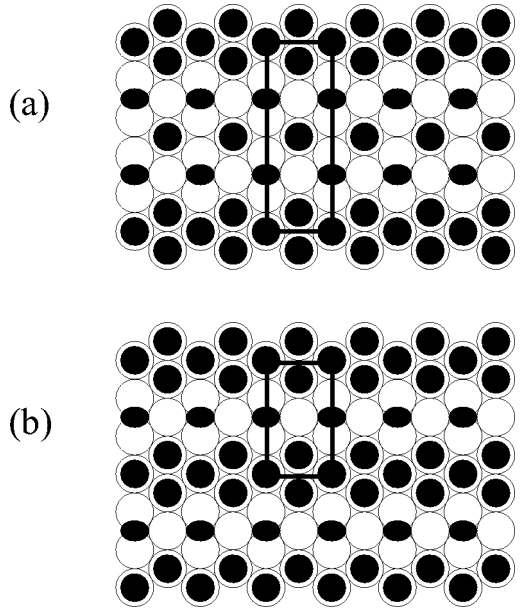

FIG. 1. High coverage structures proposed by Avery. Domains of half-monolayer $c(4\times2)$ are separated by fault lines composed of top CO molecules at full monolayer coverage. Circles represent atop CO molecules and ovals represent bridge-bonded CO molecules. (a) Coverage of 0.6 ML with $(\sqrt{3}\times5)$ periodicity. (b) Coverage of 0.667 ML with $(\sqrt{3}\times3)$ periodicity

Above 0.5 ML, surface crowding and CO-CO repulsion might be expected to lead to off-normal bonded CO molecules on Pt(111). Kiskinova, Szabo, and Yates measured electron stimulated desorption ion angular distributions (ESDIAD) to study high CO coverages on the Pt(111) surface.[32] Three species were detected desorbing from the surface. The triplet CO* and positive ion CO^+ trajectories reflect the Pt-C bond angle while CO^+ trajectories give information about the C-O bonds. The authors demonstrated that high coverage CO/Pt(111) phases are associated with tilted atop CO species with a tilting angle of up to $6\pm1°$ from the normal, as indicated by the CO* species or up to $14\pm1°$ as indicated by the CO^+ species. The CO^+ species is strongly influenced by image charge and neutralization effects at large angles and therefore the polar angle of the atop bonded CO species was concluded to be $\sim6°$, as indicated by the CO* species.[32]

III. METHODS

The main goal of our research has been to describe the potential energy profile for a CO molecule adsorbing on the Pt(111) surface with varying amounts of CO precoverage. Using DFT, we have performed geometry minimizations in which the C atom of an adsorbing CO molecule was fixed at

a specific point along the surface normal. The energies of the constrained minimizations describe a potential energy curve for adsorption of the CO molecule. All degrees of freedom for the C and O atoms except for the *z* coordinate of the adsorbing C atom were unconstrained. In order to determine the binding energy for CO at the minimum of the potential energy curve, a minimization in which all C and O atoms were unconstrained was also performed for each model. While we have computed the binding energy for various configurations of CO on the Pt(111) surface, we would like to emphasize that our overall goal is not to calculate the binding energies but to investigate the barriers to adsorption.

The DFT calculations were performed with the Vienna *ab initio* simulation package (VASP),[33,34] and made use of the projector augmented wave (PAW) method of Blöchl.[13,14] The plane-wave basis set included waves up to 400 eV. We used the Perdew and Zunger[35] parametrization of the local exchange-correlation functional according to the quantum Monte Carlo simulations of Ceperley and Alder,[36] adding nonlocal corrections in the form of the generalized gradient approximation (GGA) as presented by Perdew *et al*.[37]

The GGA (LDA, experimental) values for the bulk modulus and lattice constant are 2.39 (3.10, 2.78) Mbar and 3.99 (3.92, 3.92) Å , respectively, in good agreement with previous DFT studies.[38] The GGA value for the cohesive energy of -6.05 eV/atom is lower than the value of -7.52 eV/atom calculated using the LDA (Ref. 38) and when it is compared to the experimental value of -5.84 eV/atom, the GGA represents an improvement over the LDA.

Three supercells were considered: a $(\sqrt{3}\times 2)$ supercell, with four Pt atoms per layer, a $(2\sqrt{3}\times 2)$ supercell with eight Pt atoms per layer, and a $(\sqrt{3}\times 3)$ supercell with six Pt atoms per layer; in all cases the CO was adsorbed on only one side of the slab model. In order to estimate the error due to using a four layer slab, $(\sqrt{3}\times 2)$ supercells with three, four, and five layers were considered; changing from three to four layers changes the surface energy for the bare, ideal surface by only 0.029 eV/(1×1) unit cell and changing from four to five layers changes the same quantity by only 0.017 eV/(1×1) surface cell.

A vacuum layer of five layers was introduced to separate the slabs. Increasing the vacuum layer to eight layers changes the surface energy by 0.0003 eV/(1×1) surface cell. Brillouin-zone integrations were performed on a grid of $8\times 7\times 1$, $(4\times 6\times 1, 7\times 4\times 1)$ *k* points for the $(\sqrt{3}\times 2)$, $(2\sqrt{3}\times 2)$, and $(\sqrt{3}\times 3)$ supercells, respectively. For the $(2\sqrt{3}\times 2)$ supercell, calculations were performed on a series of grids up to a $6\times 8\times 1$ grid to verify that the energies are converged with respect to *k*-point sampling. On increasing from the $4\times 6\times 1$ to a $6\times 8\times 1$ grid, the total energies change by less than 0.015 eV.

To accelerate the *k*-point convergence, a generalized Gaussian smearing according to Methfessel and Paxton was adopted with order one and a width of 0.2 eV.[39] Minimum energy structures were obtained by minimization of the forces according to a quasi-Newton (variable metric) algorithm.[40]

During relaxations, the platinum atoms were kept fixed at bulk positions. Relaxation of the platinum atoms leads to changes in the surface energy on the order of 0.001 eV/(1×1) surface cell for the $(\sqrt{3}\times 2)$ supercell. The binding energy for the $c(4\times 2)$-2CO phase increases by 75 meV per molecule when the substrate Pt atoms are allowed to relax. While it would be interesting and valuable to calculate the binding energies and barriers to adsorption with relaxation of some of the substrate Pt layers, the calculational effort involved was judged to be in excess of the available computational resources.

IV. CO ADSORPTION ON PT(111)

Calculations were carried out for various possible adsorption models as pictured in Fig. 2 and summarized in Table I.

A. CO adsorption at low CO coverage

Using a $(\sqrt{3}\times 2)$ supercell, we have calculated a low-dimensional potential energy profile for CO adsorption from 0.0 to 0.25 ML. The approaching molecule is placed in a vertical position with the C-atom pointing downwards directly above the intended adsorption site. As the distance from the surface is gradually decreased, only the Pt atoms and the height of the carbon atom are kept fixed during the optimizations. The adsorption model is shown in Fig. 2(a) and the potential energy as a function of the C-atom height is shown in Fig. 3. We have modeled CO adsorption at the top site. The calculated binding energy is 1.55 eV, which is in good agreement with calorimetric experimental results.[16,17] As can be seen in Fig. 3, the calculations predict no barrier to adsorption at low CO coverage.

Our calculations predict no tilt of the CO molecule, in agreement with experiment.[32] Our calculated model gives a C-O bond length of of 1.156 Å (compared to 1.128 Å in the gas phase) and a Pt-C bond length of 1.865 Å.[41]

B. CO adsorption at medium CO coverage

Using a $(2\sqrt{3}\times 2)$ supercell, we calculated the potential energy profile for adsorption from 0.375 to 0.5 ML in two cases. In the first case the CO molecule descends onto a top site; see Fig. 2 (b). In the second case the CO molecule is adsorbing onto a bridge site; see Fig. 2 (c). In both cases, the final coverage pattern corresponds to the $c(4\times 2)$-2CO phase.

Our converged structures for the $c(4\times 2)$-2CO phase have CO bond lengths of 1.154 and 1.185 Å for atop and bridge-bonded CO molecules, respectively. For the atop CO, our predicted bond length differs from experiment by less than 4% and for the bridge-bonded CO, the agreement is better than 1%.[31] The calculated C-Pt distances are 1.872 and 1.465 Å , for atop and bridge-bonded CO molecules, respectively, which are within 10% of the experimentally measured values.[31] Our model does not allow for the relaxation of the Pt atoms, which undoubtedly contributes to the latter discrepancies. The CO molecules in our calculated model are aligned parallel with the surface normal, again in agreement with experiment.[31]

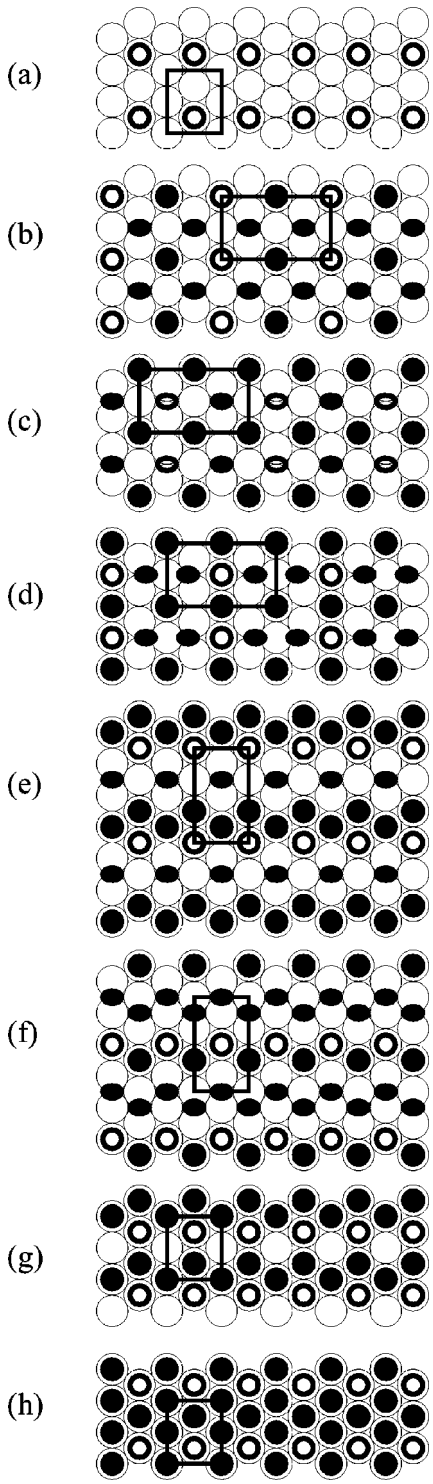

FIG. 2. Models for CO adsorption on Pt(111): (a) ($\sqrt{3}\times2$) supercell, 0.000 to 0.250 ML, (b) ($2\sqrt{3}\times2$) supercell, 0.375 to 0.500 ML, (c) ($2\sqrt{3}\times2$) supercell, 0.375 to 0.500 ML, (d) ($2\sqrt{3}\times2$) supercell, 0.500 to 0.625 ML, (e) ($\sqrt{3}\times3$) supercell, 0.500 to 0.667 ML, (f) ($\sqrt{3}\times3$) supercell, 0.500 to 0.667 ML, (g) ($\sqrt{3}\times2$) supercell, 0.500 to 0.750 ML, (h) ($\sqrt{3}\times2$) supercell, 0.750 to 1.000 ML. Filled circles represent preadsorbed atop CO molecules and ovals represent bridge-bonded CO molecules. Open symbols represent adsorbing CO molecules. Refer to Table I.

The potential energy profile for adsorption at the top (bridge) site is plotted in Fig. 4 using filled (empty) symbols. There is no calculated barrier for adsorption at either the top or the bridge site. The binding energy for the atop CO molecule is calculated to be 1.52 eV while the binding energy for the bridge-bonded CO molecule is 1.61 eV. The difference between these binding energies is not significant, given the site preference problems that are known to exist for DFT descriptions of CO on Pt(111).[8]

C. CO adsorption at high CO coverage

Starting with the ordered $c(4\times2)$ 0.5 ML structure, we calculated the potential energy profile for bringing in another CO molecule over the central Pt atom. For this adsorption process, the coverage changes from 0.5 to 0.625 ML. In this case, to accommodate the incoming CO molecule, the two preadsorbed bridge-bonded CO molecules slide laterally away from the central Pt atom of the ($2\sqrt{3}\times2$) supercell [see Fig. 2 (d)].

The potential energy profile for model (d) as well as those for models (e) and (f) are shown in Fig. 5. Here we calculate a small (0.10 eV) barrier to adsorption. The binding energy for the adsorbed atop CO molecule is only 0.96 eV, a significant decrease from the lower coverage scenarios. We have compared the density of states (DOS) for adsorption on the clean surface with the DOS for adsorption on the precovered surface; shifts in the DOS were observed but no clear pattern was identified. We suggest that the barrier to adsorption for CO on the CO-precovered surface could arise from Pauli repulsion between the arriving CO molecule and those already on the surface, as this is consistent with the shifts observed in the DOS.

Using the ($\sqrt{3}\times3$) supercell pictured in Fig. 2(e), we have modeled adsorption from 0.5 to 0.667 ML. Model (e) is the 0.667 ML coverage version of the ''compression'' structures proposed by Avery [see Fig. 1 (b)] and is composed of strips of half-monolayer $c(4\times2)$ separated by strips of full ML coverage.[24] Our calculations predict, in the strip of full monolayer coverage, CO-CO repulsive interactions lead to off-normal or tilted CO molecules, in agreement with the ESDIAD results of Kiskinova *et al.*[32] Model (e) has one bridge-bonded, two tilted atop CO molecules, and one untilted atop CO molecule in the ($\sqrt{3}\times3$) supercell. We have modeled adsorption of one of the tilted CO molecules (see Fig. 5). For this process there is a slight (0.13 eV) barrier to adsorption and the calculated absorption energy is 1.15 eV.

Our calculations indicate the angle of the tilted CO top molecules in model (e) to be 13°. In their ESDIAD study, Kiskinova and co-workers measured an angle of $14\pm1°$ as indicated by the CO^+ species while the the CO* species indicated an angle of only $6\pm1°$. However, the CO^+ species is strongly influenced by image charge and neutralization effects in the ESDIAD experiment and therefore the true tilting angle of the CO molecule was concluded to be closer to $6\pm1°$ from the normal, as indicated by the CO* species.

It is conceivable that the same problems that lead to the site-preference problems in DFT for CO on Pt could also contribute to an overestimation of the CO tilting angle in

TABLE I. CO adsorption models: θ_i and θ_f denote initial and final coverage in ML, respectively, $\overline{E_{\mathrm{ads}i}}$ and $\overline{E_{\mathrm{ads}f}}$, denote the average binding energy per adsorbed CO molecule for the initial and final structures (in eV), site denotes position at which CO adsorption occurs, $t{:}b{:}h$ is the number of top-, bridge- and hollow-site bonded CO molecules in the model, C-O is the bond length for the adsorbed molecule, E_{act} is the activation energy (in eV), and E_{ads} is the binding energy (in eV) for the adsorbed CO molecule. Refer to Fig. 2.

Model	Supercell	θ_i	$\overline{E_{\mathrm{ads}i}}$	θ_f	$\overline{E_{\mathrm{ads}f}}$	Site	$t{:}b{:}h$	C-O	E_{act}	E_{ads}
a	$(\sqrt{3}\times 2)$	0.000	0.00	0.250	1.55	top	1:0:0	1.156	0.00	1.55
b	$(2\sqrt{3}\times 2)$	0.375	1.60	0.500	1.58	top	2:2:0	1.154	0.00	1.52
c	$(2\sqrt{3}\times 2)$	0.375	1.57	0.500	1.58	bridge	2:2:0	1.185	0.00	1.61
d	$(2\sqrt{3}\times 2)$	0.500	1.58	0.625	1.46	top	3:2:0	1.154	0.10	0.96
e	$(\sqrt{3}\times 3)$	0.500	1.46	0.667	1.38	top	3:1:0	1.158	0.13	1.15
f	$(\sqrt{3}\times 3)$	0.500	1.43	0.667	1.39	top	2:2:0	1.157	0.03	1.27
g	$(\sqrt{3}\times 2)$	0.500	1.44	0.750	1.13	top	3:0:0	1.158	0.49	0.50
h	$(\sqrt{3}\times 2)$	0.750	1.13	1.000	0.92	top	4:0:0	1.159	0.58	0.30

DFT calculations. The Blyholder model describes bonding between CO and Pt atoms as a mixture of two effects: donation from the 5σ molecular orbital of the CO to the d_{z^2} orbital of the metal atom and back donation from the d_{xz} and d_{yz} orbitals of the metal to the $2\pi^*$ antibonding orbital of the CO molecule.[11,23,42–44] Both interactions are favorable, but the first interaction favors bonding of the CO at the top site while the second favors bonding at higher coordination hollow sites, specifically because overlap between the d_{xz} and d_{yz} orbitals of the metal and the $2\pi^*$ orbital of the CO is enhanced.[11] Kresse has argued that the site preference problem of current DFT functionals springs from the fundamental underestimation of the HOMO-LUMO gap, which leads to an overestimation of the interaction between the d_{xz} and d_{yz} orbitals of the metal and the $2\pi^*$ orbital of the CO.[11] When atop CO molecule is tilted, there is logically an increase in overlap between the d_{xz} and d_{yz} orbitals of the metal and the $2\pi^*$ orbital of the CO; this of course is accompanied by an equal decrease in overlap on the other side and a cancellation of any effect. In model (e), tilting of the atop CO molecules is favored because of a repulsive effect between CO molecules in close proximity. It is possible that the abovementioned overemphasis on the (favorable) interaction between the d_{xz} and d_{yz} orbitals of the metal and the $2\pi^*$ orbital of the CO in current DFT methods could result in an overestimation of the tilt angle.

It is interesting to compare the results for models (d) and (e). In both cases, initial coverage is $\frac{1}{2}$ ML, although the configurations differ. In both cases, a relatively small (0.10–0.13 eV) barrier to adsorption is predicted. In both cases, adsorption of CO at a top site is modeled. For model (d) the calculated energy of adsorption for the final coverage of $\frac{5}{8}$ ML is lower than that of model (e), which has a final coverage of $\frac{2}{3}$ ML. This is in contrast to the general trend in which adsorption energy decreases as coverage increases. [An increase in CO adsorption energy with preadsorbed O has also been observed on Ru(0001).[45]] This result indicates that model (e) is more likely than model (d) to describe adsorption of CO on Pt(111) at high coverage, in agreement with experiment.[24,29,32]

We also performed calculations for a model proposed by Biberian *et al.* for the $(\sqrt{3}\times 3)$ unit cell.[26] This model is identical to that proposed by Avery except that the registry between the adsorbate and the metal differs [compare Fig. 1(b) and Fig. 6]. In the case of Avery's structure, there are three atop and one bridge-bonded CO molecule. The structure proposed by Biberian *et al.* has three bridge-bonded and one atop CO. Our calculations indicate that this structure is not, in fact, a stable energy minimum, and therefore we will not present further results for it.

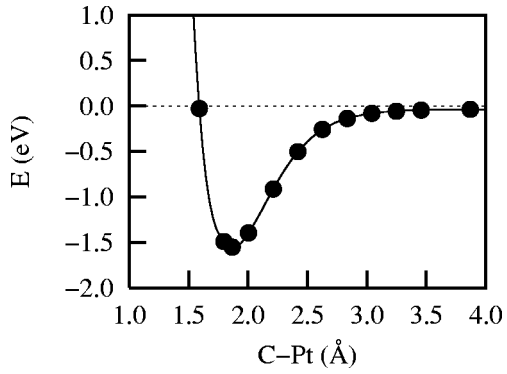

FIG. 3. Potential energy profile for model (a): adsorption of CO at a top site from 0.00 to 0.25 ML.

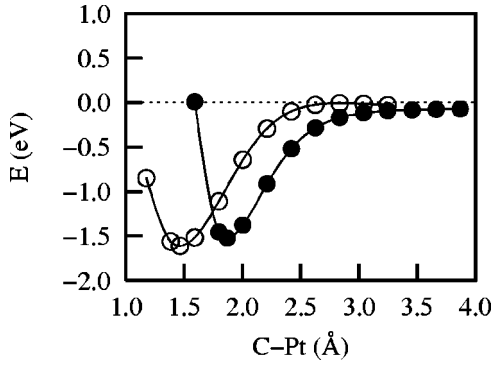

FIG. 4. Potential energy profile for models (b) and (c): adsorption of CO from 0.375 to 0.500 ML, top site (filled symbols) and bridge site (empty symbols), respectively.

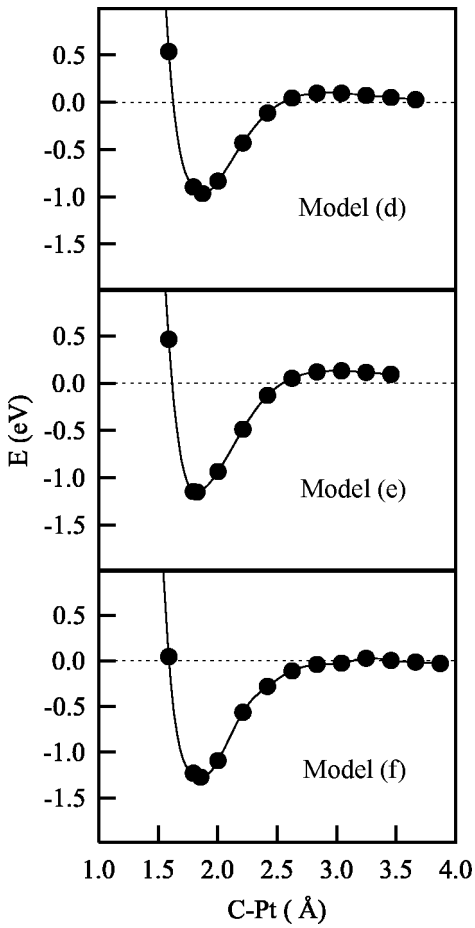

FIG. 5. Potential energy profile for models (d): adsorption of CO at top site from 0.500 to 0.625 ML and for models (e) and (f): adsorption of CO at top site from 0.500 to 0.667 ML. Models (e) and (f) differ in the patterns of the preadsorbed CO molecules (see Fig. 2).

We have calculated the potential energy profile for adsorption of CO from 0.5 to 0.667 ML for yet another adsorption pattern [see Fig. 2 (f)]. This model of adsorption is similar to model (e), proposed by Avery, in that the periodicity is $(\sqrt{3}\times 3)$, the initial coverage is $\frac{1}{2}$ ML, the final coverage is $\frac{2}{3}$ ML and adsorption of CO at a top site is modeled. The difference is that two of the three preadsorbed CO molecules are at bridge sites, instead of one of the three, as was the case for model (e). The final configuration of 0.667 ML consists of zig zag rows of CO molecules with half adsorbed on top sites and half adsorbed on bridge sites [see Fig. 2 (f) and Fig. 5].

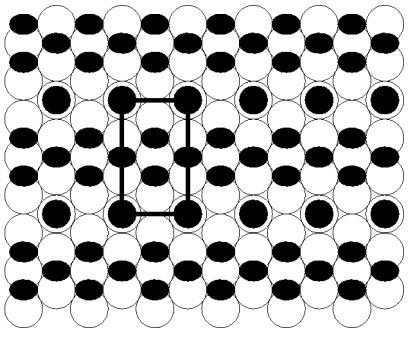

FIG. 6. High coverage structure proposed by Biberian *et al.* for the $(\sqrt{3}\times 3)$ unit cell (see text). Our calculations indicate that this structure is not a minimum on the potential energy surface.

TABLE II. Calculated and experimental vibrational frequencies (ν, cm^{-1}) and intensities (I, arbitrary units), for CO adsorbed on Pt(111) according to models (e) and (f) described in the text. Experimental values are taken from Ref. 24.

Model	ν	I
Experiment	2100	1.00
	1870	0.35
Model (e)	2079	1.00
	2020	0.01
	2012	0.03
	1822	0.17
Model (f)	2088	1.00
	2041	0.00
	1890	0.22
	1840	0.01

Our calculations indicate this arrangement to be even more favorable for CO adsorption, as there is an almost nonexistent barrier to adsorption (0.03 eV) and the calculated energy of adsorption is 1.27 eV, in excellent agreement with the calorimetric measurement of 1.22 eV by Yeo *et al.* at ''saturation coverage.''[20] The minimum energy structure for model (f) predicts a C-O bond length of 1.157 Å for the atop molecules and 1.180 Å for the bridge-bonded molecules. The atop molecules are nearly aligned with the surface normal but the bridge-bonded molecules are tilted with respect to the surface normal by approximately 7°. This angle is quite close to the 6° reported by Kiskinova *et al.*[32]

In order to compare our high-coverage structures with the available experimental results, we have calculated the vibrational modes of CO adsorbed on Pt(111) according to models (e) and (f). In our calculations we have allowed all degrees of freedom for the C and O atoms but held all Pt atoms fixed. The second derivative of the Hamiltonian was estimated from the forces according to the finite difference approach. We used two displacements per atom, each of 0.04 Å, to estimate the second derivatives.

In Table II, we present calculated frequencies for these models. We present only the four CO stretching modes (all other calculated modes for both models are below 500 cm^{-1}). We have estimated the intensities in proportion to the square of the calculated dynamic dipole moments, scaled by the intensity of the strongest mode for each model.

The EELS experiments[24] performed in the high-coverage limit show the most intense stretching frequency (attributed to atop CO) at $\sim$2100 cm^{-1}, followed by a second stretching mode of about one-third of the intensity at $\sim$1870 cm^{-1} (assigned to bridge-bonded CO). Our calculations for model (e) and (f) agree with experiments in predicting the highest intensity for the CO stretch vibrations of atop-adsorbed CO. The calculated frequencies agree with experiment to within

1–1.5 %. The models differ significantly in the frequency with the second largest intensity; model (f) leads to a mode with 22% of the maximal intensity at 1890 cm^{-1}, for model (e) a mode with comparable intensity is found only at a much lower frequency of $\sim$1820 cm^{-1}. This mode is attributed to the CO stretch of the bridge-bonded species.

In our calculation of the $c(4\times2)$-2CO phase, for which refined structural data has been reported,[31] our calculated bridge-bonded CO bond length is 1.185 Å. The bond length for the bridge CO for this phase as determined by tensor LEED is 1.19 Å, meaning that our calculations have slightly underestimated the bridge-bonded CO bond length. This is in contrast to the CO bond length of the atop CO species, which is overestimated slightly by our calculations. An underestimated bond length will generally lead to an overestimated frequency and vice versa. Thus, the best match to experiment should be the model that gives a too-low frequency for the top CO species and a too-high frequency for the bridge-bonded CO species. Therefore, between these two models, model (f) is the better match with experiment.

It is useful to compare the results for modeling adsorption from 0.5 to 0.667 ML according to models (e) and (f). Model (e) (proposed by Avery) is composed of strips of half-monolayer $c(4\times2)$ separated by strips of full ML coverage and has three top CO molecules and one bridge-bonded CO molecule.[24] Model (f) is composed of zig-zag lines of CO molecules with half bonded on top and half on bridge sites. The tilt angle for CO on model (e) is predicted to be 13° while that for model (f) is 7°, which is in better agreement with the ESDIAD results of Kiskinova and co-workers.[32] In model (e), the tilted CO is an atop-bonded species while in model (f) it is the bridge bonded species. The adsorption energy for model (e) is 1.15 eV, in reasonable agreement with experiment, but that for model (f) is 1.27 eV, which is in even better agreement with the experimental value of 1.22 eV.[20] The calculated barrier for adsorption for model (e) is 0.13 eV, which is not large, but the value for model (f) is only 0.03 eV. Finally, the calculated adsorbate frequencies for model (f) are in better agreement with experimental results. Therefore, a comparison of the calculated energies, geometries (CO tilt angles), and adsorbate vibrational frequencies for models (e) and (f) suggests that model (f) is a better description of the adsorption structure in the high coverage limit.

D. CO adsorption at coverages beyond 0.667 ML

Finally, for completeness, we present the potential energy profile for adsorption from 0.5 to 0.75 ML [see Fig. 2 (g)] and from 0.75 to 1.0 ML [see Fig. 2 (h)] using a $(\sqrt{3}\times2)$ supercell with all CO molecules on top sites. The potential energy profiles for both models are presented in Fig. 7.

For model (g), there is a significant barrier to adsorption (0.49 eV) and the calculated binding energy is only 0.50 eV. Here the calculated barrier is almost as large as the energy of adsorption. It is unlikely that this scenario accurately models adsorption of CO on Pt(111) at high coverage.

For model (h) the adsorption results in full monolayer coverage of CO on Pt(111), the barrier to adsorption rises to 0.58 eV and the calculated adsorption energy decreases to 0.30 eV. The calculations predict the formation of full monolayer coverage structure to be (slightly) exothermic, but the barrier to adsorption is larger than the energy of adsorption. This is consistent with the fact that complete monolayer coverage has not been experimentally observed.

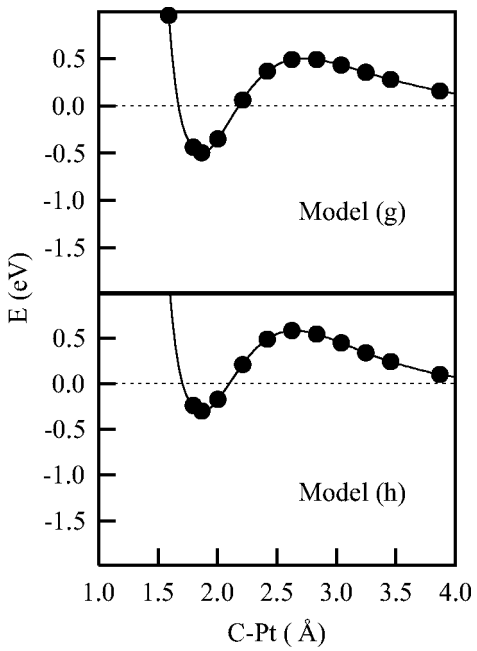

FIG. 7. Potential energy profile for models (g) and (h), adsorption of CO from 0.500 to 0.750 ML and from 0.750 to 1.00 ML, respectively.

V. CONCLUSIONS

Standard *ab initio* calculations of molecular adsorption on solid surfaces are usually concerned with interaction of an adsorbate layer representing a specified surface coverage with the initially clean surface. In many cases exothermic adsorption energies are calculated for coverages exceeding

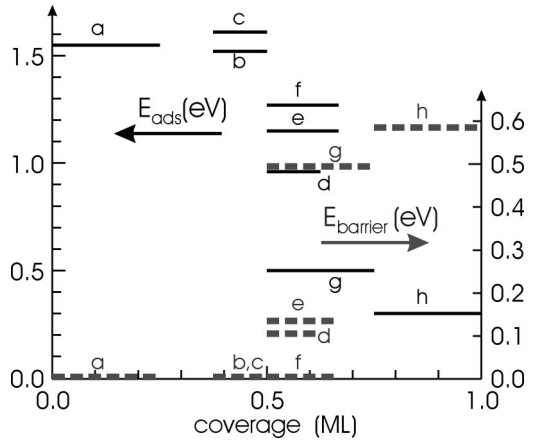

FIG. 8. Adsorption energies (black lines) and barriers (gray dashed lines) for all calculated models. The lines stretch from the initial coverage to the final coverage reached after adsorption of the impinging molecule.

the saturation coverage determined experimentally. While a few attempts have been made to account for the influence of preadsorbed species on the adsorption energies, no systematic theoretical investigation of the variation of the potential energy surfaces of impinging molecules as a function of the precoverage of the surface by the same species has been performed.

In the present work we have modeled the gradual formation of a CO adlayer of increasing density on a Pt(111) surface. Starting from the clean metal surface we have constructed a series of models for CO/Pt(111) adsorption layers and calculated the potential energy profile for molecules impinging on a precovered surface. It is clear that the simultaneous addition of a substantial fraction of a monolayer is only a moderately realistic picture of the adsorption process. Hence the calculated energy profiles should be considered only as a reasonable approximation to the most favorable adsorption channels for a specific coverage.

Figure 8 summarizes the results for adsorption energy and barrier height. The results show that even up to a precoverage of 0.5 ML, the adsorption energy for impinging molecules decreases only slightly and that adsorption remains an unactivated process. For coverages exceeding $\frac{2}{3}$ ML the situation changes very rapidly. The adsorption energy decreases steeply and a substantial barrier builds up. At coverages of close to $\frac{2}{3}$ ML, the stable adsorption geometry is still a subject of debate. Different models consisting of crowded strips with all Pt atoms covered by top adsorbed CO have been proposed. Our calculations suggest that model (f), with an equal number of top- and bridge-adsorbed CO, is energetically preferred over model (e), a structure with a majority of top-adsorbed CO but a stronger contrast between very dense and rather dilute areas. This conclusion is also supported by the analysis of the vibrational spectra. A useful extension of this work would be to consider adsorption of CO to form the $c(\sqrt{3}\times 5)$ model for 0.6 ML coverage proposed by Avery [see Fig. 1 (a)] which we have not considered in this paper.[24]

ACKNOWLEDGMENTS

This work was supported by the Austrian Science Funds within the Joint Research Project ''Gas-Surface Interactions'' (Grant No. S8106-PHYS).

*Present address: National Energy Technology Laboratory, United States Department of Energy, P. O. Box 10940, Pittsburgh, PA, 15236-0940. Email address: steckel@netl.doe.gov

[1] M. M. Schubert, M. J. Kahlich, H. A. Gasteiger, and R. J. Behm, J. Power Sources **84**, 175 (1999).
[2] B. Hammer, Y. Morikawa, and J. K. Nørskov, Phys. Rev. Lett. **76**, 2141 (1996).
[3] B. Hammer, O. H. Nielsen, and J. K. Nørskov, Catal. Lett. **46**, 31 (1997).
[4] A. Alavi, P. Hu, T. Deutsch, P. L. Silvestrelli, and J. Hutter, Phys. Rev. Lett. **80**, 3650 (1998).
[5] A. Eichler and J. Hafner, Surf. Sci. **433**, 58 (1999).
[6] A. Eichler and J. Hafner, Phys. Rev. B **59**, 5960 (1999).
[7] M.Ø. Pedersen, M.-L. Bocquet, P. Sautet, E. Lægsgaard, I. Stensgaard, and F. Besenbacher, Chem. Phys. Lett. **299**, 403 (1999).
[8] P. J. Feibelman, B. Hammer, J. K. Nørskov, F. Wagner, M. Scheffler, R. Stumpf, R. Watwe, and J. Dumesic, J. Phys. Chem. **105**, 4018 (2001).
[9] I. Grinberg, Y. Yourdshahyan, and A. M. Rappe, J. Chem. Phys. **117**, 2264 (2002).
[10] A. Gil, A. Clotet, J. M. Ricart, G. Kresse, M. García-Hernández, N. Rösch, and P. Sautet, Surf. Sci. **530**, 71 (2003).
[11] G. Kresse, A. Gil, and P. Sautet, Phys. Rev. B (to be published).
[12] B. Hammer, L. Hansen, and J. K. Nørskov, Phys. Rev. B **59**, 7413 (1999).
[13] P. E. Blöchl, Phys. Rev. B **50**, 17 953 (1994).
[14] G. Kresse and D. Joubert, Phys. Rev. B **59**, 1758 (1999).
[15] C. Lu, I. C. Lee, R. I. Masel, A. Wieckowski, and C. Rice, J. Phys. Chem. A **106**, 3084 (2002).
[16] D. A. Kyser and R. I. Masel, J. Vac. Sci. Technol. A **4**, 1431 (1986).
[17] D. A. Kyser and R. I. Masel, Rev. Sci. Instrum. **58**, 2141 (1987).
[18] F. Thomas, N. Chen, I. Lee, L. Ford, P. Blowers, and R. I. Masel, J. Vac. Sci. Technol. A **17**, 2339 (1999).
[19] W. T. Lee, L. Ford, P. Blowers, H. L. Nigg, and R. I. Masel, Surf. Sci. **416**, 141 (1998).
[20] Y. Y. Yeo, L. Vattuone, and D. A. King, J. Chem. Phys. **106**, 392 (1997).
[21] W. A. Brown, R. Kose, and D. A. King, Chem. Rev. (Washington, D.C.) **98**, 797 (1998).
[22] G. Ertl, M. Neumann, and K. M. Streit, Surf. Sci. **64**, 393 (1977).
[23] J. V. Nekrylova, C. French, A. N. Artsyukhovich, V. A. Ukraintsev, and I. Harrison, Surf. Sci. Lett. **295**, L987 (1993).
[24] N. R. Avery, J. Chem. Phys. **74**, 4202 (1981).
[25] M. Kiskinova, A. Szabo, and J. T. Yates, Jr., J. Chem. Phys. **89**, 7599 (1988).
[26] J. P. Biberian and M. A. V. Hove, Surf. Sci. **138**, 361 (1984).
[27] D. F. Ogletree, M. A. V. Hove, and G. A. Somorjai, Surf. Sci. **173**, 351 (1986).
[28] H. Steininger, S. Lehald, and H. Ibach, Surf. Sci. **123**, 264 (1982).
[29] K. L. Kostov, P. Jakob, and D. Menzel, Surf. Sci. **377**, 802 (1997).
[30] F. Bondino, G. Comelli, F. Esch, A. Locatelli, A. Baraldi, S. Lizzit, G. Paolucci, and R. Rosei, Surf. Sci. **459**, L467 (2000).
[31] I. Zasada and M. A. V. Hove, Surf. Rev. Lett. **7**, 15 (2000).
[32] M. Kiskinova, A. Szabo, and J. T. Yates, Jr., Surf. Sci. **205**, 215 (1988).
[33] G. Kresse and J. Furthmüller, Phys. Rev. B **54**, 11 169 (1996).
[34] G. Kresse and J. Furthmüller, Comput. Mater. Sci. **6**, 15 (1996).
[35] J. P. Perdew and A. Zunger, Phys. Rev. B **23**, 5048 (1981).
[36] D. M. Ceperley and B. J. Alder, Phys. Rev. Lett. **45**, 566 (1980).
[37] J. P. Perdew, J. A. Chevary, S. H. Vosko, K. A. Jackson, M. R. Pederson, D. J. Singh, and C. Fiolhais, Phys. Rev. B **46**, 6671 (1992).
[38] A. Kokalj and M. Causá, J. Phys.: Condens. Matter **11**, 7463 (1999).
[39] M. Methfessel and A. T. Paxton, Phys. Rev. B **40**, 3616 (1989).

[40] P. Pulay, Chem. Phys. Lett. **73**, 393 (1980).
[41] G. Herzberg, *Molecular Spectra and Molecular Structure*, 2nd ed. (Van Nostrand, New York, 1979), vol. 4.
[42] G. Blyholder, J. Phys. Chem. **68**, 2772 (1964).
[43] H. Aizawa and S. Tsuneyuki, Surf. Sci. **399**, L364 (1998).
[44] A. Föhlisch, M. Nyberg, J. Hasselström, O. Karis, L. G. M. Pettersson, and A. Nilsson, Phys. Rev. Lett. **85**, 3309 (2000).
[45] C. Stampfl and M. Scheffler, Phys. Rev. B **65**, 155417 (2002).